H2020 Grant Agreement No. 730562 – RadioNet

PROJECT TITLE:	Advanced Radio Astronomy in Europe
STARTING DATE	01/01/2017
DURATION:	48 months
CALL IDENTIFIER:	H2020-INFRAIA-2016-1
TOPIC:	INFRAIA-01-2016-2017
	Integrating Activities for Advanced Communities

Deliverable 5.1

SIS Junction mixer operating around 1THz

Due date of deliverable: 2019-06-30

Actual submission date: 2019-12-03

Leading Partner: THE CHANCELLOR, MASTERS AND SCHOLARS OF THE UNIVERSITY OF OXFORD (UOXF)

Document information

Document name:	Reports on the development of SIS tunnel junctions and SIS mixers at 1.0 THz
Type	Report
WP	WP5 – AETHRA
Version date:	2019-12-03
Authors (Institutes)	Ghassan Yassin (UOXF)
	Andrey Baryshev (RUG)
	Netty Honigh (UCO)

Dissemination Level

Dissemination Level		
PU	Public	X
PP	Restricted to other programme participants (including the Commission Services)	
RE	Restricted to a group specified by the consortium (including the Commission Services)	
CO	Confidential, only for members of the consortium (including the Commission Services)	

Table of contents

1 Executive Summary

The successful operation of a high-performance SIS mixers at THz frequencies requires the development of state-of-the-art technology in several areas including device development, mixer chip design, development and fabrication of feeds, and micro-machining of mixer blocks. In addition, cryogenic receiver systems need to be built to test these mixers and theoretical tools and simulations need to be developed in order to analyse their performance. At such high frequencies it is desirable that the RF signal is launched inside the cryostat to avoid absorption by water lines and losses in warm optical components. Also, because of thin film processing restrictions, high gap superconducting tunnel junctions are often used. These junctions may comprise complex layer structure consisting of different materials. This gives rise to phenomena such as heating of the device as a result of trapping of normal electrons at the boundaries, which needs to be explored and understood. Finally, the mixer mechanical components such as feeds and waveguide transitions are extremely tiny (of the order of 100 micron) which makes their fabrication and integration to the mixer block very challenging.

In our yearly reports, we have reported excellent progresses in both device development and mixer design and testing. In what follows, we will report on the progress of this work and how it was utilized for the design and testing of THz SIS mixers in the frequency range of ALMA band 10 (780-950 GHz). The achievements of the team may be summarized as follows:

1. The University of Cologne (UCO) can now to reproducibly fabricate Nb-AlN-NbN SIS tunnel junctions with a current density of at least 25 kA/cm2 and a gap voltage around 3.5 mV. Junction Areas of 0.6 μm2 can be made reliably. The precision of the actual area definition is not better than ±25% but for areas equal to or larger than 0.6 μm2 the area size is very consistent over the wafer. The presently fabricated SIS junctions are embedded into normal metal wiring. For embedding into superconducting wiring UCO will need to do more process optimization, which goes beyond the scope of the present contract. The last year of the contract will be dedicated to fabricating mixer devices, evaluated at 1.4 THz. Observations at this frequency range is possible by ALMA (band 11) and also by CCAT-p observatory which is being built at the Andes at an altitude of 5600 m and UCO is a collaborator in this project.

2. At the University of Groningen (RUG) they have developed an SIS mixer operating in the frequency range of 780-950 GHz. The mixer chip structure, mechanical design and electromagnetic design were made in at RUG. The mixer employed Nb/AlN/NbN devices that were fabricated at Institute of Radio Engineering and Electronics IREE in Moscow. The devices have an energy gap of 3.15 mV (compared to 2.8 mV measured for Nb) and a high current density of 30 kA/cm2. The device was tested by RUG in an ALMA style mixer block and obtained noise temperature of 300-500 K in an IF bandwidth of 4-12 GHz.

3. At the University of Oxford (UOXF) we have constructed a THz mixer test system with optics and cold load inside the cryostat. The mixer view can be switched from hot (300 K) to cold (4K) loads using a cryogenic stepper motor. We have used this system to test an SIS device that we obtained from RUG, which was fabricated using the same process and characteristics to the device tested at RUG (Nb/AlN/NbN). We have compared the performance of the device with loads inside and outside the cryostat and demonstrated the advantages when the loads and optics are installed inside the cryostat. This work was carried in collaboration with RUG. We have also designed and tested smooth-walled THz feed horns for both UOXF and RUG mixers. A new batch of THz mixer has also been designed and is currently in the process of fabrication at Paris Observatory (OBSPARIS).

4. We have performed thorough analysis of the performance of the mixer that was tested by UOXF and RUG. In particular we have demonstrated that the suppression of the superconducting gap is indeed the result of heating of the tunnel junction by LO RF signal and DC bias and investigated the effect of heating on the performance of the mixer. This work is still in progress and a summary will soon be submitted for publication before the end of the year.

5. We have developed smooth-walled feed-horns that are easy to fabricate at THz frequencies. These feeds have low-sidelobes and excellent beam circularity and yet can be milled directly into a block of aluminium (or cooper) avoiding the need for electroforming (see section 1.4.1). These feeds have already been implemented in CMB instruments [1]

6. We have written a software package for rigorous design and analysis of SIS mixers. The description of the software packages has already been published and the software package was made publicly available [2].

In summary, we have achieved the development of state-of-the-art SIS mixer technology including SIS devices that can potentially operate at frequencies above 1.3 THz and developed an SIS mixer at ALMA band 10 that gave noise temperature of 300-500 K in the frequency range of 780-950 GHz.

2   Design, Fabrication and Testing of THz SIS Mixers

2.1   Development of THz NbN SIS Devices

As it is well known, the superconducting gap of niobium (Nb) in unit of frequency is approximately 700 GHz. However, the theory of quantum mixing guarantees that SIS mixers can work at frequencies well above the gap. It is therefore evident that SIS mixers in the ALMA band 10 frequency range can work well using Nb devices (and in fact the present ALMA band 10 mixer does use a Nb junction). Care of course needs to be taken in designing the transmission lines since niobium is very lossy above the superconducting gap hence the ALMA band 10 mixer uses a normal metal for the required transmission lines (such as the tuning circuits).

In the present work however, we have chosen to work with materials whose superconducting gap is above the 2.8 meV of niobium (this is a typical value at 4 K). The reason for that is because developing devices above 3.0 meV is both scientifically interesting and has the added important advantage that the same devices will be available for future mixers operating at higher frequencies, in particular in the ALMA band 11 window centred at 1.3 THz.

In this work we have developed and tested SIS devices with Nb and NbN electrodes and AlN barriers (NbN/AlN/NbN), achieving high quality I-V curves with a superconducting gap of 3.5 meV in one fabrication process and a superconducting gap of 3.15 meV in another. In the second case the device was successfully operated as a THz SIS mixer. A summary of this work is given below.

2.1.1   Development of THz SIS devices at UCO

UCO has managed to reproducibly fabricate Nb-AlN-NbN SIS junctions with a current density of a least 25 kA/cm2 and a gap voltage around 3.5 mV. An IV curve of one of the devices is shown in *Fig. 2.1-1*. Devices with junction areas of 0.6 μm^2 can be made reliably and sometimes even a few 0.3 μm^2 area junctions succeed. The precision of the actual area definition is not better than ±25% but for areas of 0.6 μm^2 and larger the area size is very consistent over the wafer. This gives us the possibility to arrive at the right resonance frequency for the integrated tuning-circuit by employing a ±25% variation of design frequency over the wafer. In addition, as the definition of devices will be done with E-beam lithography, we will be able to easily adjust the dimensions from one wafer to the next.

The presently fabricated SIS junctions with the specifications as mentioned above are all embedded into normal metal wiring. When embedded in superconducting wiring, using the NbTiN, the SIS junction reproducibility was not as good. These devices might be suitable for frequencies around 1 THz, depending on the THz properties of the NbTiN which should be determined separately, but we would need to do more process optimization, and possibly   implement an interface layer of a normal metal (e.g. Au) between the NbTiN-wiring and junction electrodes. This puts this activity, time wise, beyond the scope of the present contract.

With normal metal tuning-circuits we will not be competitive at frequencies close to 1 THz but it makes the frequency band of 1.2 -1.5 THz available for SIS mixers for the first time. In this frequency band observations from the ground are still possible in atmospheric windows that can be seen by the new CCAT-p observatory. This observatory is presently being built at a height of 5600m at the Andes and UCO is part of this project.

As UCO has already finished the development of the SIS junctions we are now in position to fabricate the mixer. We decided to make a relatively simple mixer with a resonant integrated tuning that is comparatively insensitive to fabrication tolerances. The main research objective of this mixer is to determine the mixing properties of our SIS junctions.

UCO will choose to make a waveguide mixer because some parts (horns) for this frequency range are already available from a previous project and we have expertise in making waveguide mixers at frequencies up to 4.7 THz. The waveguide mixer blocks will be fabricated in house and are in essence a scaled version of UCO blocks at higher frequencies.

The tuning structures are designed, and a signal coupling between 20% and 40% is expected, resulting in a margin of a factor of 2 in the predicted noise temperature. The actual coupling depends critically on the SIS junction current density (RnA product) and on the THz-conductivity of the normal metal leads that form the resonant tuning circuit. It is the goal to separate these influences as well as possible from the mixing properties of the SIS junction that are the primary research objective.

Therefore 30% of the fabrication wafer area is dedicated to test structures to determine current density and normal metal properties. The current density of the SIS junction will be determined from the DC IV curves of a number of test-junctions with different (larger) areas at 2 separated areas of the wafer. Test structures to determine the THz properties of the normal metals, at cryogenic temperatures, are currently being designed, to finalize the fabrication set.
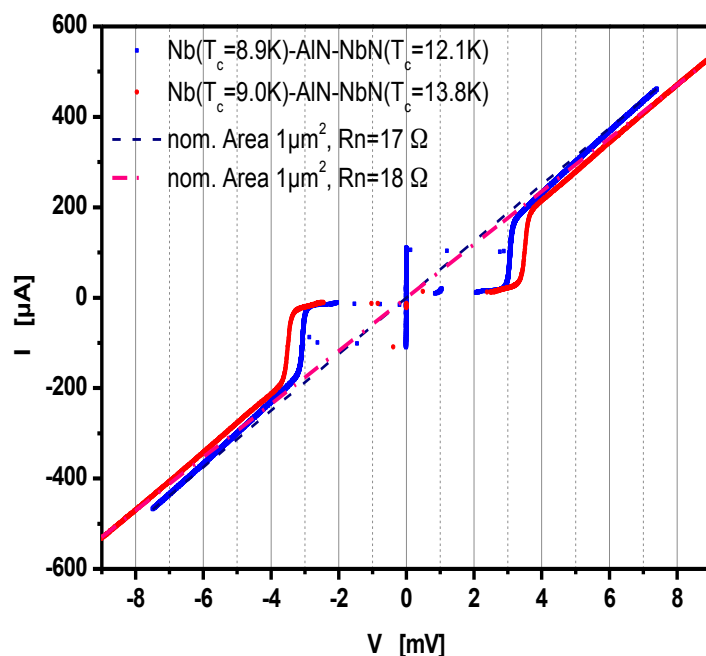

Fig. 2.1-1 DC IV-curves of 2 SIS junctions fabricated at UCO with an area of 1 μm^2, measured at 4.2K in liquid helium. The red and blue curves show the IV-curves of Nb-AlN-NbN SIS junctions from 2 different fabrication wafers. It shows the reproducibility of the current density and the control of the gap voltage by the optimization of the critical temperature (T) of the NbN junction electrode

2.1.2 Development of THz SIS devices at RUG

RUG has developed critical current-density Nb/AlN/NbN tunnel junctions incorporated in microstrip line consisting of a 300-nm-thick bottom electrode (ground plane) made of NbTiN and a 500-nm-thick top electrode made of Al. The microstrip electrodes are separated by a 250-nm SiO isolator. The Nb layer of the SIS junction is deposited on the NbTiN film, while the NbN layer is contacting the Al top electrode. The details of fabrication are as follows: First, a NbTiN film was deposited on a fused quartz substrate at room temperature by dc sputtering with a NbTi target in a nitrogen atmosphere. For the NbTiN film, the critical temperature was measured to be $T_c = 14.1$ K, and room temperature resistivity estimated to be 85 $\mu\Omega$.cm. The tunnel junctions were fabricated from a Nb/AlN/NbN tri-layer with a normal-state resistance–area product $7\Omega.\mu m^2$, which corresponds to a current density of 30 kA/cm^2. The Nb and NbN layers have thicknesses of 100 nm. Circular-shape junctions with an area of about 0.5 μm^2 were defined by deep ultraviolet photolithography. The SIS junctions were patterned from the Nb/AlN/NbN tri-layer by successive RIE of the NbN layer using CF4, by RF sputtering of AlN/Al film in Ar plasma and finally by RIE of Nb layer using CF4 . The dielectric layer for junction insulation consists of 250-nm SiO, defined in a self-aligned lift-off procedure. At the final step, a 500-nm-thick top microstrip electrode made of Al was deposited by dc magnetron sputtering. Afterwards, the thickness of the quartz substrate was thinned to 40 μm by mechanical polishing.

The frequency of 950 GHz corresponds to 3.9-mV photon step, which exceeds both our fabricated SIS junctions and of course the classical ones with Nb electrodes (2.8 mV). Our junction however provides a wider voltage range available for SIS mixer biasing by about 0.7 mV. This gives a big advantage for the mixer operation due to the presence of the problematic Shapiro feature right at the middle of the photon step (can be seen in *Fig. 3.2-2*). Due to the high current density of the produced AlN barrier, the lower R_n gives a higher $1/CR_n$ ratio for the junctions, providing a wider receiver bandwidth.

3 Development of THz SIS mixers

3.1 Development of feeds for THz mixers

An important component for a high-quality THz mixer is the feed that couples the radiation from the telescope optics to the mixer chip effectively. A good mixer feed needs to have low return loss (better than –20 dB), low cross polarization (better than –20 dB), low sidelobes level and good beam circularity (identical E- and H-plane patterns down to less than –10 dB).

UOXF has pioneered the development of a new class of THz feed-horns, the multiple flare-angle smooth-walled horn, which has comparable performance to corrugated horn and yet is much easier to fabricate. A large number of horns can be fabricated rapidly and simultaneously by repeated milling into a single aluminium block using a shaped machine tool. The principle of operation is based on creating several discontinuities in flare angle along the horn to excite a balance of fundamental and high-order modes. If the magnitudes and locations of these discontinuities are carefully chosen, the mode combination propagates down the horn with the correct phase would give a highly uniform field distribution across the aperture and a radiation pattern with low sidelobes and cross polarization. The positions and the magnitudes of the discontinuities are determined using an UOXF-developed software package (`HornSynth`) that combines mode matching analysis and genetic algorithm optimisation. Alternatively, one can design these feeds using the **TICRA®** software package `CHAMP®`, which featured the multiple flare-angle smooth-walled horn as an example in their manual.

Using `HornSynth`, we have optimized the design of three smooth-walled sections feeds to operate from 780-950 GHz (in line with the frequency range of the RUG NbN mixer described above). A schematic diagram of this horn is shown in *Fig.   3.1-1*, and the horn dimensions are given in Table

3.1-1. From the simulated and measured radiation patterns shown in *Fig. 3.1-2*, it can be seen that the horn produces a good beam circularity across the whole band with a maximum cross polarisation peak at approximately –25 dB at 945 GHz. As well as this, the radiation patterns show very low side lobe levels and high beam efficiency.
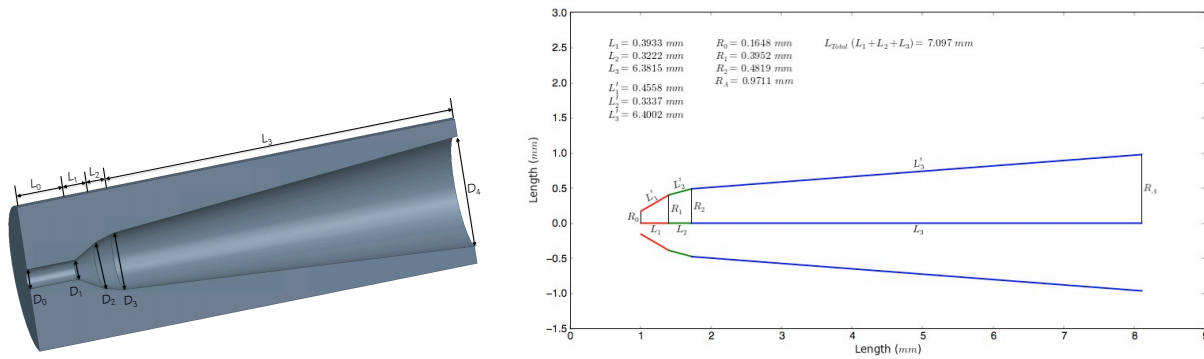

Fig. 3.1-1 Schematic diagram of a 3 section, 850 GHz smooth walled horn.

Table 3.1-1 The dimensions defining the inner wall of the THz feed horn.

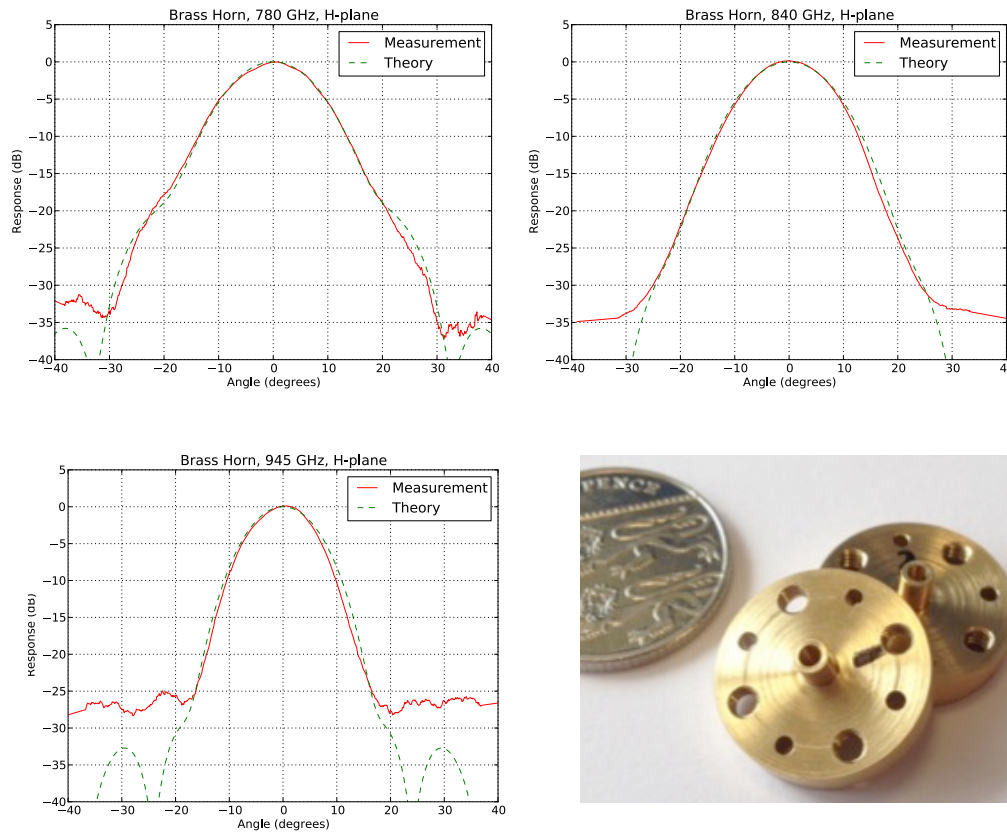| Dimension	Length (mm)
R_0	0.1762
R_1	0.4102
R_2	0.5236
R_A	0.14682
L_1	0.4278
L_2	0.4259
L_3	10.2241

Fig. *3.1-2 Simulated and measured radiation patterns at 780, 840 and 945 GHz, along with the photo of the THz feed horn.*

From the radiation patterns shown above we can see excellent agreement between theory and experiment. We would like to emphasise that the flattening of the measured pattern at 945 GHz below −25 dB is the result of the finite dynamic range of the measurement system at the high frequency end.

3.2 Development of a pulsed tube test system with internal loads

We have constructed and optimised the performance of a heterodyne receiver system designed to operate at frequencies ~THz for testing of high frequency SIS mixers. The RF optics, including the beam splitter, focusing mirrors and hot/cold loads are mounted inside the cryostat. Only the LO source is located outside the vacuum environment, where the LO signal is injected though the cryostat window, as shown in *Fig. 3.2-1*. The bare cryostat was built by Janis Research Company, using a pulsed tube cooler to cool the working area down to 2.9 K (without any thermal loads). *Fig. 3.2-1* shows the picture of the cryostat and the experimental arrangement inside the working area. All the components shown in the figure (b) are fabricated in house at UOXF, apart from the cryogenic stepper motor and the mixer block. Before we embarking on testing the THz mixers with the system, we fully characterised the system using an existing 700 GHz mixers with known performance, allowing us to discover various unexpected systematic problems. This includes the electronic grounding of the system, unknown source of external electrical pulses that blowing up SIS devices, and distortion of the dielectric beam splitter surface during the cooling process. Nevertheless, we have successfully mitigated all these problems, and the system is currently operational and has been used routinely to test the THz SIS mixer.
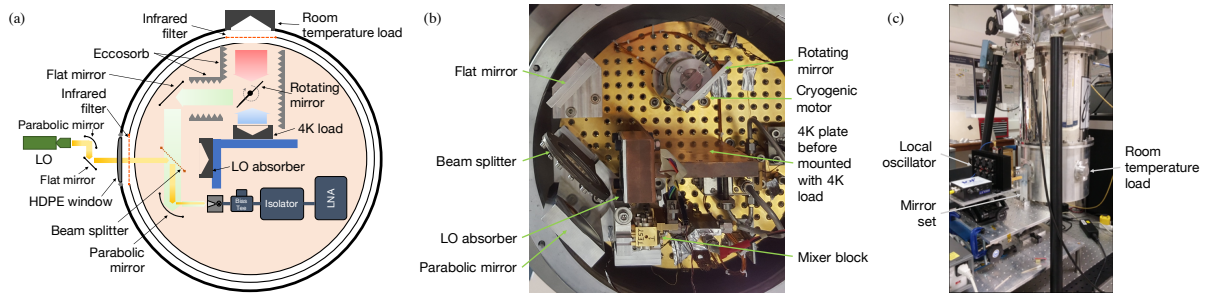
Fig. 3.2-1 (a) Schematic layout of the internal optics of the cryostat. (b) Image showing the actual optical setup. (c) A photo showing the external LO setup along with the PTC cryostat.

For measuring the noise temperature of the SIS mixers, we used the standard Y-factor methods by illuminating the mixer with blackbody loads at different physical temperature. The room temperature (300 K) load was mounted on the outer wall of the cryostat (via a window socket, as shown in *Fig. 3.2-1* (c)), while the 4 K load was attached to a 4 K plate anchor mounted on the cold plate (see *Fig. 3.2-1* (b)). We used a rotating mirror mounted on top of a cryogenic stepper motor to sweep between the hot and cold load to perform the Y-factor measurements. LO power was coupled from outside the cryostat to the mixer using a Gaussian telescope arrangement via another optical window. This optical arrangement with the entire RF path housed within the vacuum environment ensures that the effect of the water absorption is minimized, thus allowing us to assess the actual performance of the mixer near THz frequencies.

Fig. 3.2-2 (a) shows an example of the DC current-voltage (IV) curves (pumped and unpumped) and the intermediate frequencies (IF) responses of the SIS mixer, when the mirror is stationary and facing either the hot or the cold blackbody load. *Fig. 3.2-2* (b) shows the IF output of the SIS mixer biased at around 2.4 mV, when the rotating mirror is swept around in a full rotation period. It shows clearly the difference in IF responses when the mixer is illuminated with a hot (room temperature) and the 4 K cold load. The feature near 60 degrees is the case when the mirror is directing the beam straight back to mixer horn, hence setting up a standing wave that reflects the LO power back to the mixer. Note that we enshroud the RF path with Eccosorb® absorber to reduce the multiple reflections inside the cryostat that would contaminate the measurement, and the backside of the mirror is also coated with absorber (hence the flat IF output from 180-360 degree in the plot).
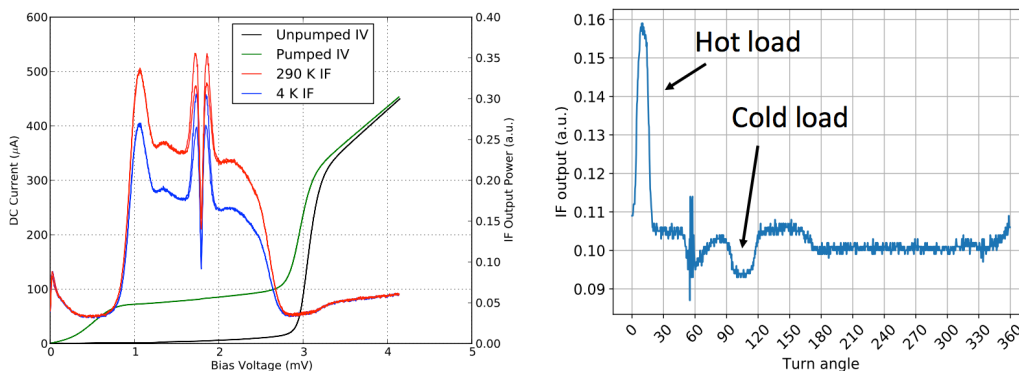

Fig. 3.2-2 a) measured pumped and unpumped IV curves, along with the hot and cold IF responses, at 850 GHz. (b) The IF response of the mixer when the mirror is swept along its rotational axis, pointing the mixer beam towards different surfaces within the cryostat, including the room temperature hot and 4 K cold load. The mixer was biased at 2.4 mV and the LO set at 850 GHz.

3.3 Mixer tests at RUG

The SIS mixer chip employed by RUG uses a design of twin junction tuning structure and waveguide similar to the one used by CHAMP+. The SIS junctions are embedded in a 4.5 µm wide microstrip line and separated by 6.5 µm and coupled to the antenna by a 7x27 µm [3]. The mixer block design is similar to the ALMA mixer block and used a half waveguide to couple power to the probe.

Noise temperature was measured by the Y-factor method using room temperature (300 K) absorber as hot load and absorber immersed in liquid nitrogen (77 K) as a cold load. The results of the noise temperature measurements are depicted in *Fig. 3.3-1*. The data is corrected for the 88% transparent 12- µm mylar beam splitter used for LO injection. Each point on the graph represents the DSB (dual sideband) noise temperature averaged over a 4–12-GHz intermediate frequency band. For the best junctions, the level is about 230 K at low frequencies, and it goes up to 550 K at high frequencies. The RF frequency range was limited by the availability of LO power. Nevertheless, the noise temperature was measured at 680 GHz and 720 GHz using a different LO source, yielding values of 900 K and 350 K, respectively, confirming the extremely wide RF range of the mixer (exceeding 200 GHz). In general, the measured is in good agreement with FTS measurements that we performed before the noise temperature testing.
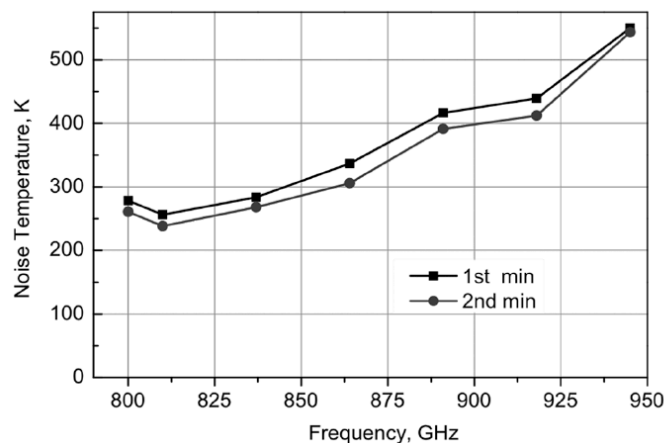

Fig. 3.3-1 Measurement of the noise temperature of the THz SIS mixer at RUG. The noise temperature is corrected for LO insertion beam splitter and measured at the first (square) and second (circles) minima of the Josephson current.

During the experiments, we found it difficult to suppress the Josephson critical current of twin sub-micron SIS junctions. This problem arises due to shape and area difference between the junctions. For better suppression, it is preferable to use the second or even the third minimum of the critical current curve (Josephson current versus magnetic field), since these minima are shallower than the first. However, it is known that a too-high magnetic field reduces the gap voltage and can even decrease the response of the mixer at high frequencies; both effects have a negative influence on the mixer performance.

3.4 THz mixer performance tests at UOXF

3.4.1 Noise temperature measurement

We have performed extensive noise temperature tests at ALMA Band 10 frequency range using the RUG device described above. The mixer assembly we used for the tests was designed such that a separate back-piece housing the SIS device could be bolted to the same mixer block for quick turn-around testing. The SIS device-loaded back-piece and part of the mixer block were supplied by the

Kapteyn Astronomical Institute (RUG) group to Oxford, where the rest of the mixer block including the feed-horn and the circular-to-rectangular waveguide transition were fabricated at Oxford Physics workshop. The back-piece and the transition were aligned to the output of the feed horn and held in place using a threaded centring ring. The whole assembly (horn + mixer) was then slotted into an Atacama Large Millimetre/Sub-Millimetre Array (ALMA)-style mixer block, which contains a temperature sensor, magnetic coils and the DC/IF SMA connector. This resulted in an SIS mixer identical to the one tested at RUG excluding the feed horn and circular to rectangular waveguides transition.

We have measured the noise temperature of the THz mixer with the standard Y-factor method using both the traditional (external loads) approach and internal loads of our THz system. The external load measurements were performed by replacing the 300 K load (mounted on the window port of the cryostat body, see *Fig. 3.2-1*(c)), with a "transparent" window. The rotating mirror was fixed at a position that directed the mixer beam towards the window, where the hot and cold (absorber dipped with liquid nitrogen at 77 K) loads were used to illuminate the mixer from outside the cryostat manually. The measurements with the external loads were performed to act as a bench-mark to internal loads measurements that will follow.

Since these measurements were taken at the frequency range of approximately 775–935 GHz and in the "internal loads" case used a cold load of ~4K, the Rayleigh-Jeans (R-J) approximately could not be used for estimating the blackbody temperature, alternatively, the Callen-Welton (C-W) formula was used to recover the effective blackbody temperature. For example, with a cold load at the physical temperature of 4K, the effective blackbody temperature is calculated to be 18.6 K at 775 GHz and 22.4 K at 935 GHz, almost 5 times higher than the R-J approximation. The C-W correction was not used when evaluating the hot (300 K) and cold (77 K) external load since the R-J approximation is clearly valid at these temperatures.

During the measurements, we were initially unable to recover the same noise temperature (T_N) measured by the RUG group with a similar mixer chip from the same fabrication batch, particularly at a certain frequency intervals where the noise temperature peaked to about 3–4 times higher. The effect of water vapour absorption was ruled out since the RF path of our system is enclosed in a vacuum environment. By carefully inspecting the IF output of the mixer, we noticed that the total power output at these frequency ranges increased unexpectedly, leading us to believe that the increase in T_N was in fact caused by excessive noise injected from the LO into the mixer. We later verified that the source of these increase of the LO noise was caused by the synthesiser used to drive the LO multiplier chain. At near THz frequencies where the LO is formed via a cascade of several multiplier stages, it turns out that the multiplier chain is extremely sensitive to the phase noise produced by the microwave synthesiser. We therefore built a dedicated microwave source using a YIG oscillator to replace the general-purpose signal synthesiser, and successfully removed the extra noise introduced by the LO source.

The results of our measurements, both with internal and external loads, are shown in *Fig. 3.4-1* (left). The noise temperature calculated with the internal loads is on average ~75 K lower than that calculated with external loads at the same frequency, which is expected taking into account the RF loss of the "transparent" window used in the case of external loads. This exercise demonstrates that our THz mixer measurement system is now performing well and calibrated for further mixer tests.
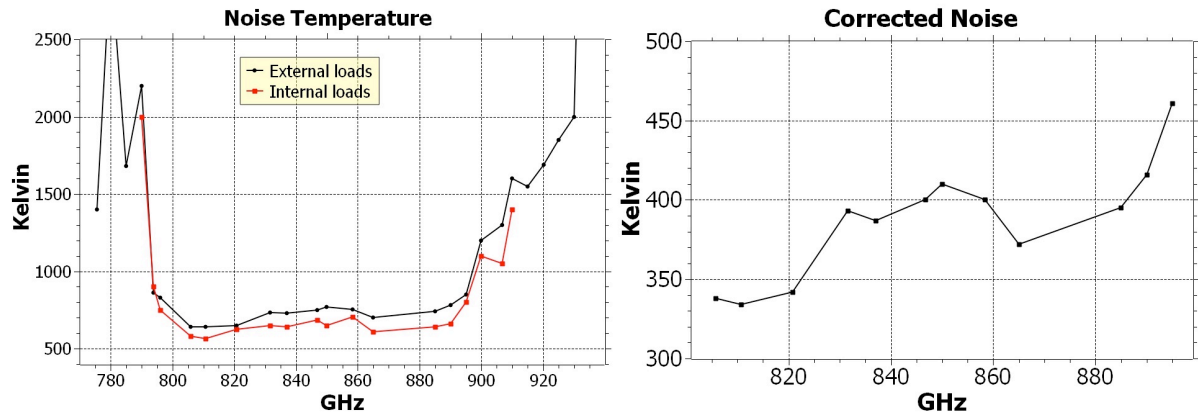
Fig. 3.4-1 Uncorrected T_n calculated with the standard Y-factor method. The average difference in T_n between the internal and external loads is about 75 K (Left). Noise temperature corrected for the beam splitter loss and waveguide mismatch (Right).

Fig. 3.4-1 (left) shows that the TN measured at UXOF is much higher than that measured by the RUG group (see Section 3.3). This is however mainly caused by the waveguide mismatch between our circular-to-rectangular waveguide transition fabricated at UOXF and the RUG supplied SIS device loaded backpiece, which uses half-height waveguide backshort. In the original RUG mixer assembly, the feed horn block was electro-formed with the corrugated horn and the circular-to-rectangular waveguide fabricated in a single piece. However, to avoid the need for the complex electroforming and to take advantage of the ease of fabricating the smooth-walled horns, we fabricated our feed horn by direct drilling with a separate circular-to-rectangular full-height waveguide transition. The performance of the smooth-walled horn has been reported earlier in Section 3.1 and has shown to have comparable high-quality performance as the corrugated horn. But because the circular-to-rectangular waveguide transition used by our horn ended up with full waveguide height and the back-piece supplied by RUG has half-height waveguide, this resulted in a strong mismatch that needed to be corrected in order to obtain a better assessment of the sensitivity of our mixer. Using rigorous electromagnetic simulations to assess the effect of this mismatch, we estimate that the power transmission could have been reduced by ~40% in some frequency range.

Furthermore, our LO was designed to operate at wider frequency range, at the expense of lower output power. Therefore, we need to increase the LO coupling to the mixer by 1) aligning the E-field of the RF propagation vertical to the plane of reflection and 2) using a thicker beam splitter. The results are shown in *Fig. 3.4-1* above were measured with a 19 um beam splitter. Consequently the measured noise temperature performance was corrected for the losses introduced by the waveguide mismatch and the beam splitter. The corrected noise temperature plot is shown in *Fig. 3.4-1* (right) and is now comparable to the performance measured at RUG to within 50 K. The mixer sensitivity is calculated at about 2.8–4.6× quantum limit (double side band, DSB) and the mixer gain is estimated at about –4 to –6 dB in the frequency range reported above. We would like to stress that the waveguide mismatch and the beam splitter loss were estimated via simulations; hence the precision of the results reported here can be further improved by eliminating the mismatches.

In order to further understand the behaviour of the THz mixer, we attempted to separate the RF and IF noise contributions to the total noise temperature performance. Using the standard IF calculations, we estimate the IF chain contribution to be around 8–10 K. This leads to the conclusion that most of the noise arises from the RF components before the mixer. Using the intersection line method (using the plotting method proposed by Tong et. al. [4], we find that the RF noise contribution is in the region of about 400 K. Note that in this calculation, we do not correct for the waveguide mismatch and beam splitter loss. Nevertheless, this implies that the noise contribution from the SIS mixer is approaching 200 K (as can be seen from *Fig. 3.4-2*), which is exceeded our expectation. We therefore concluded that the standard intersection method over-estimates the RF

losses in this case, due to a different behaviour of the THz mixer, which is not common in low frequency mixers. We shall summarise our findings in the following section.
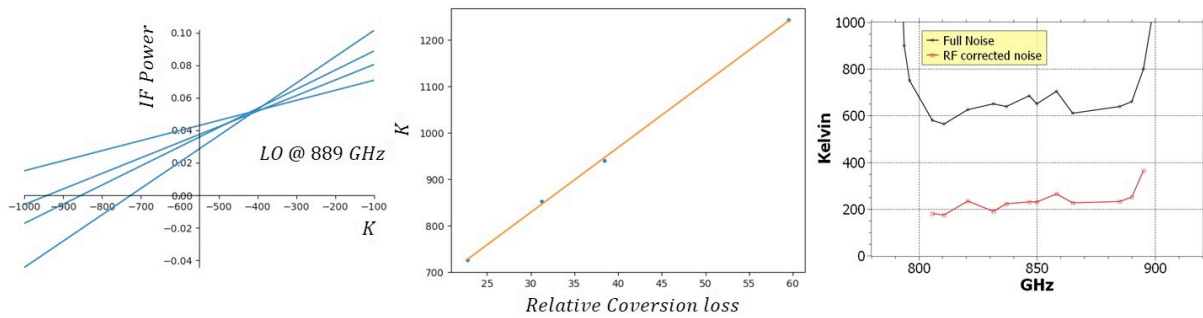

Fig. 3.4-2 Example of RF noise contribution as calculated with the standard intersection line method (Left) and the Tong, Hedden and Blundell technique (Centre) at 889 GHz. RF corrected noise compared with the uncorrected noise (Right).

3.4.2 Investigation of the effect of heating

During the characterisation of the THz mixer performance, both at RUG and UOXF it was noted that strong suppression of the gap voltage occurred when the mixer was pumped by the LO. This effect may be attributed to a local heating effect of the SIS tunnel junction, since the suppression of the gap is directly related to the increase in the physical temperature of the device. Moreover, this assumption is plausible in view of the mixer design. The tunnel junction was formed with a ground electrode of Nb and a top electrode of higher gap NbN. However, the transmission line carrying the RF signal has a NbTiN ground plane and an aluminium top wiring layer. In other words, the lower gap Nb layer is now sandwiched between two higher gap superconductors. The quasi-particles that tunnel through the barrier can therefore be trapped between the two higher-gap superconductors, thereby heating up the tunnel junction locally. This effect is clearly seen in *Fig. 3.4-3*, where the DC IV curves are plotted at different LO pumping levels. Notice that the transition gap moves towards lower bias values for higher pumping levels, demonstrating the heating effect from the LO source.
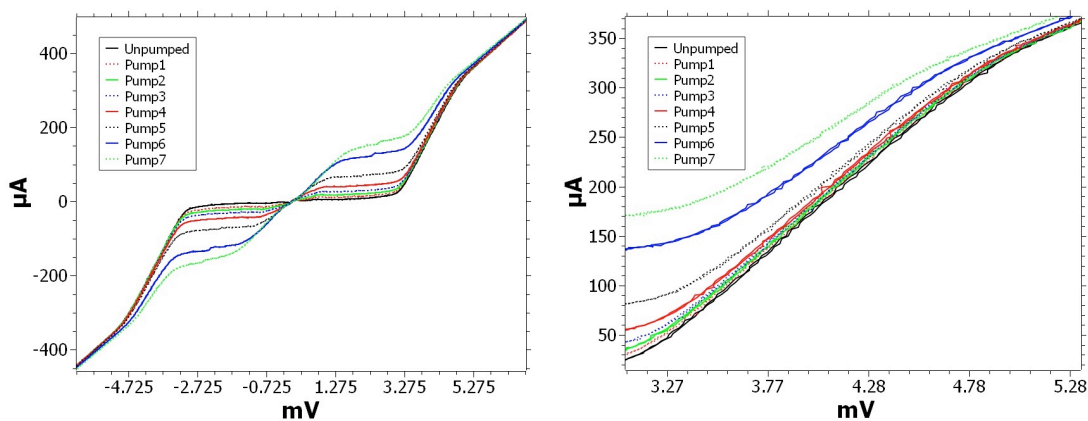

Fig. 3.4-3 IV curves for different pumping levels measured at a constant temperature (Left) and a zoom on the gap region (Right). Notice that these IV curves are not corrected for the series resistance of this particular tunnel junction hence the sloppy gap.

In order to recover the actual mixer performance without the heating effect, we need to estimate the influence of the LO power heating on the device. Fortunately, our PTC system was designed such

that we can control and stabilise the physical temperature (T_{phys}) of the cold plate (hence the mixer block), hence we estimate the heating effect temperature TLO induced by the LO. This was done by first recording unpumped IV curves at different T_{phys}, and a pumped IV curve at the lowest physical temperature (e.g. 3.22 K). Then using our mixer analysis software package [1], we generated simulated pump IV curves (using the unpumped IV curves) at different T_{phys}, and selected the one that matched the measured pumped curve. The result is shown in *Fig. 3.4-4*. The left panel shows the results of the simulated pumped IV curve using an unpumped IV curve at 3.22 K. It is clear that the simulated pumped curve does not match the measured curve. On the right panel, we show a similar plot, except that now the simulated pumped curve is calculated using an unpumped IV curve at 4.99 K. Both curves now match very well. This clearly indicated that the LO (at this pumping level) have induced an extra 1.77 K heat on the tunnel junction (i.e., TLO=1.77 K).

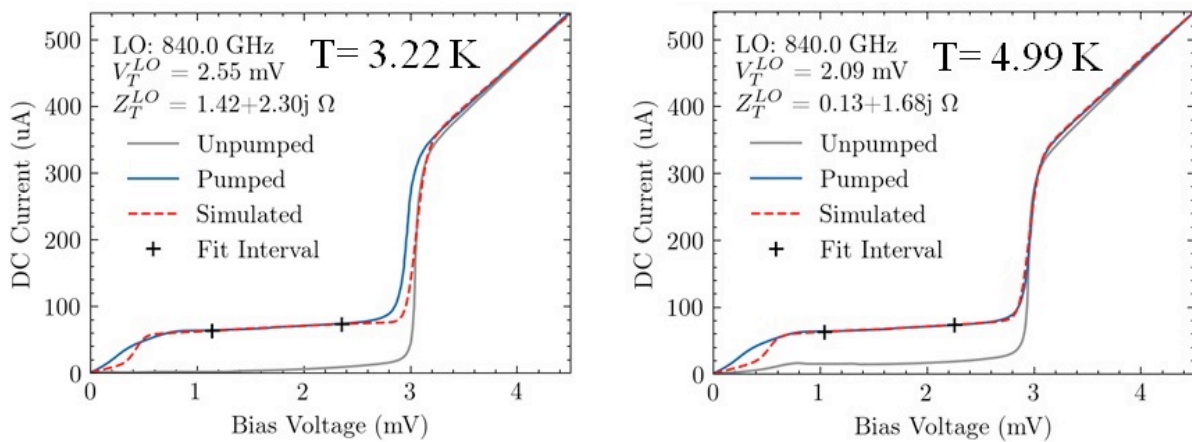*Fig. 3.4-4 Measured unpumped and pumped IV curves (solid lines) at two different temperatures Tphys, (3.22 K in the left plot and 4.99 K in the right plot), along with the corresponding simulated pumped curves (dashed red lines) produced using the measured unpumped IV curves. It can be seen from the plot that a simulated pumped IV curve based on 3.22 K unpumped IV curve cannot be recovered from the measured pump curve (left), but can be recovered from an unpumped IV curve at 4.99 K, implying that the effective temperature of the tunnel junction is in fact 4.99 K.*
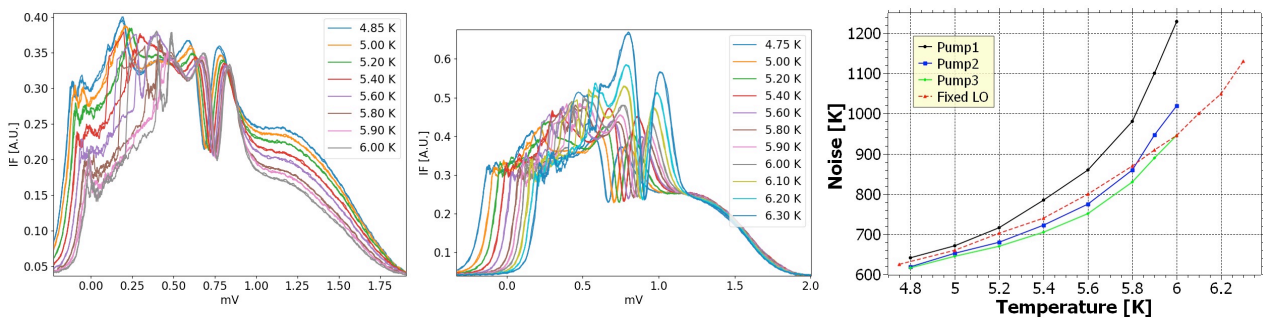

Fig. 3.4-5 IF curves at 831 GHz measured at different physical temperatures. (Left) The LO power is adjusted to keep the mixer pumping level at the same value in all cases. (Centre) The LO power is fixed. (Right) Measured mixer noise temperature as a function of the physical temperature of the mixer block.

Now it is well known that the performance of an SIS mixers vary with temperature, and in this case, both T_{phys} and T_{LO} play a part in influencing the mixer behaviour. Therefore, we need to separate the

two contributions to remove the LO heating effect and recover the actual performance of the mixer at a given bath temperature.

In *Fig. 3.4-5* (left), we show the behaviour of the down-converted IF curve (hot load) when the cold plate is set at different T_{phys} with the LO power adjusted in each case, such that the pumping is always maintained at the same level (i.e., the effective temperature is fixed $T_{phys} \uparrow$, $T_{LO} \downarrow$, $T_{eff} =$). In the centre panel, we show a similar plot, but for the case, the LO power is fixed (i.e., $T_{phys} \uparrow$, $T_{LO} =$, $T_{eff} \uparrow$).

It is interesting to note that in the first case (T_{eff} is fixed), the down-converted IF power is reduced at higher T_{phys} (from 1.0–1.5 mV). This is expected in the sense that the IF power is a function of LO power, hence lowering the LO power (to counter the effect of higher T_{phys}) produces less IF power. In the second scenario (LO power is fixed), the IF stays the same even when T_{phys} is altered. Again, since LO power stays the same, the down-converted power remains the same. It is interesting to notice a frequency dependent feature as the Fiske step near the centre of the curves is shifted towards higher bias values when T_{phys} is increased. This is due to the fact that higher T_{phys} (hence higher T_{eff}) reduces the transition gap.

Fig. 3.4-5 (right) shows the behaviour of the noise temperature T_N as a function of T_{phys} for both cases. The three solid curves represent the first case (T_{eff} is fixed) where the pumping level is fixed (by adjusting LO) power level. The dashed curve represents the second case (LO fixed). In both cases, the noise temperature deteriorated with T_{phys} as expected. However, the rate of deterioration is higher for the first case. This is because T_N is now affected both by higher T_{phys} and the lack of LO power, whereas in the second case, only by the effect of T_{phys}. In principle, this data should allow us to estimate the effect of T_{LO} on the noise mixer sensitivity and correct for it. For more accurate analysis we need to take into account the effect of leakage current caused by the increase of T_{eff}. Work is currently underway to measure the leakage current at different T_{phys} using the unpumped IV curves to remove its contribution to the pumping level.

The LO heating also influences the value of the RF noise calculated from the intersection line method described previously. This method relies on the fact that the mixer gain is a strong function of LO pump level, but the mixer noise varies only slowly with the LO below peak gain. However, as we have shown, in our case the LO level has a strong influence on the mixer noise temperature. Therefore, again we need to estimate accurately the effect of the LO heating in order to recover the RF noise contribution. An illustrative plot on how this can be done is shown in *Fig. 3.4-6*.
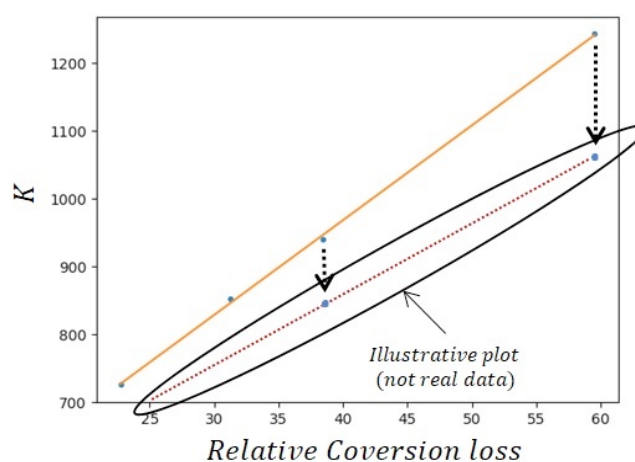

Fig. 3.4-6 Illustration of how the heating effect may interfere with the RF noise estimation technique. Orange line represents the raw measured data. It is necessary to recover the real equivalent temperature of the SIS junction at each pumping level (blue dots) in order to obtain the correct slope (dotted line).

3.5 New Mixer Design

As we explained earlier, the relatively high noise temperature we measure compared to the data from RUG (before correction) is primarily caused by the rectangular waveguide mismatch between the output of the feed horn and the back piece where the mixer is mounted. The rectangular waveguide port of the feed horn is a full-height waveguide with the narrow wall of 150 μm, in comparison to the reduced height back-piece waveguide that is half the size. We estimated that this costs about 40% losses of RF power coupling to the SIS mixer, and the situation is probably more severe when they are compounded by the conversion loss of the mixer itself.

In order to improve the performance of the SIS receiver, we have since started to modify the SIS mixer design such that it can be used with a full-height waveguide back piece, eliminating the waveguide mismatch effect. We also taken this opportunity to attempt eliminate the LO heating problem. For that, we have replaced the NbTiN ground plane with an aluminium (Al) layer, so that the hot electrons can escape via the normal metal layer. We have also replace the top-wiring layer with NbN, so that it has the same superconducting material as the top electrode of the tunnel junction. The tunnel junctions are expected to be 1 μm^2 in area, made out of Nb bottom electrode and NbN top electrode. The relatively large area junction, which strongly limits the RF bandwidth, was chosen to simplify fabrication but will be reduced at a later stage.

Fig. 3.5-1 shows the detailed design of a new mixer chip. The design is similar to the existing THz mixer, except that we replaced the triangular probe with a radial probe to cover broader bandwidth. The probe was also extended to about 35% of the waveguide height to achieve maximum coupling. A high impedance line is used to connect the radial probe to the virtual ground pad, along with the RF chokes and the IF bonding pads, forming an integrated bias-tee arrangement. We expect good noise temperature performance from 720–920 GHz, as shown in (d). We also include a design where we use a microstrip transmission line instead of stripline, and tuned slightly higher to cover the frequency range from 780–960 GHz (c) & (e).
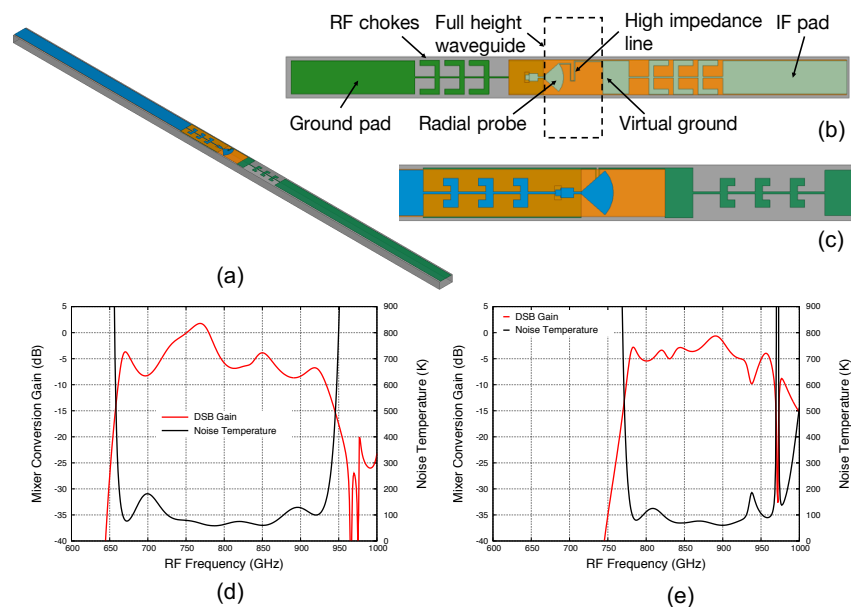

Fig. 3.5-1 (a) Illustration of the new mixer chip. (b) Mixer design similar to the existing RUG supplied mixer, except the design was altered to accommodate a full-height back short. (c) Similar to (b), but using a microstrip transmission line instead of stripline. (d) Predicted performance of the mixer (b). (e) simulated performance for (c).

In the same wafer, we have also included some end-fire antenna designs, which will have several advantages, compared to the existing design, for example less stringent requirement on the alignment tolerance between the position of the mixer chip and the waveguide. The layout of these mixer designs and their predicted performances are shown in *Fig.   3.5-2*. The mixer block and feed horn required for mounting these devices have already been fabricated. Another major advantage of these designs is that the fabrication of the circular-to-rectangular transition is straightforward since it is an integral part of the split mixer block.

We are currently in the process of fabricating these THz devices (see *Fig.   3.5-3*), in collaboration with Dr. Faouzi Boussaha from the OBSPARIS, and characterising the behaviour of the Nb/AlOx/NbN tunnel junction. We have achieved relatively high current density, but the gap voltage is still not as high as we expected, hence, work is currently in progress to understand the junction fabrication process to improve the performance.
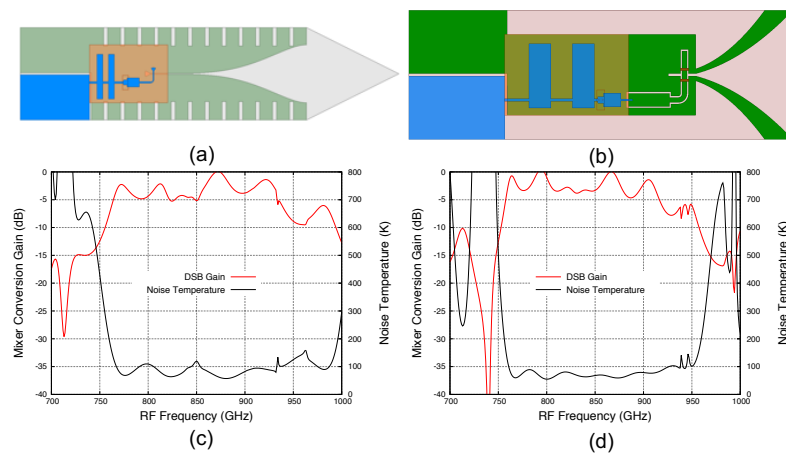

Fig.   3.5-2 (a) A THz mixer fed with unilateral finline antenna. (b) A Vivaldi antenna fed mixer. (c) Predicted bandwidth performance for the finline mixer. (d) Ditto for the Vivaldi mixer.
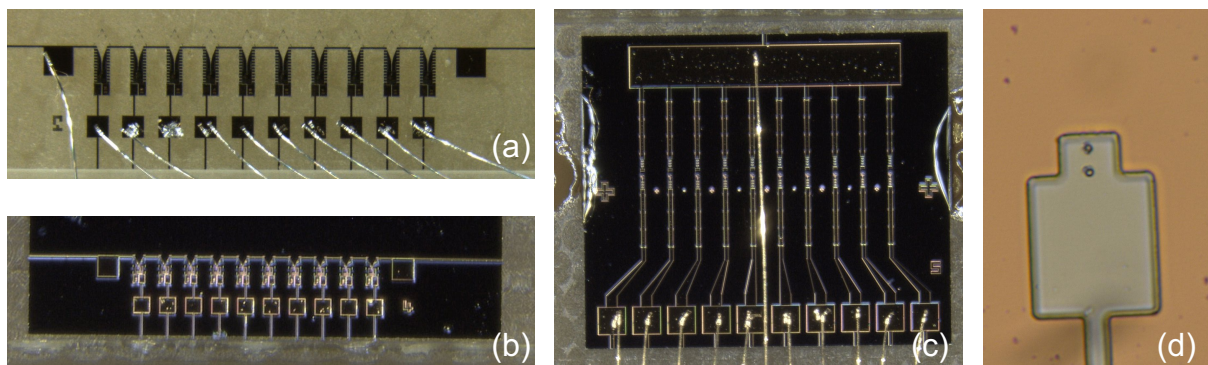

Fig.   3.5-3 Photos showing the fabricated THz mixers. (a) Finline devices. (b) Vivaldi devices. (c) Radial probe devices. (d) Zoom in image of the tunnel junctions.

4 References

[1] Dober, Bradley J., et al. "The next-generation BLASTPol experiment." *Millimeter, Submillimeter, and Far-Infrared Detectors and Instrumentation for Astronomy VII*. Vol. 9153. International Society for Optics and Photonics, 2014.

[2] John Garrette and G. Yassin "QMix: A Python package for simulating the quasiparticle tunneling currents in SIS junctions" Journal of Open Source Software, The Open Journal 4 pp. 1231-1231, 2019.

[3] Andrey Khudchenko et at "High-gap Nb-AIN-NBN SIS junctions for frequency band 790-950 GHz" IEEE Trans. THz Sci. Tech., vol. 6, pp. 127-131, 2016.

[4] C. E. Tong, A. Hedden, and R. Blundell, "An Empirical Probe to the Operation of SIS Receivers – Revisiting the Technique of Intersecting Lines," Proceedings of the Nineteenth International Symposium on Space Terahertz Technology (ISSTT), Groningen, 2008, pp. 314–318.

Copyright